

Perpendicular magnetic anisotropy and strain in Ni/Cu/Ni₆₀Cu₄₀/Cu(001)

G. Lauhoff

Toyota Technological Institute, 2-12-1 Hisakata, Nagoya 468-8511, Japan

C. A. F. Vaz and J. A. C. Bland

Cavendish Laboratory, University of Cambridge, Cambridge CB3 0HE, United Kingdom

J. Lee

ASSRC and Department of Physics, Yonsei University, Seoul 120-74, Korea

T. Suzuki

Toyota Technological Institute, 2-12-1 Hisakata, Nagoya 468-8511, Japan

(Received 28 December 1998; revised manuscript received 1 September 1999)

We report that for epitaxial Cu/Ni₆₀Cu₄₀/Cu(001) and for Cu/Ni/Cu(001) structures, the in-plane lattice parameter (a_{in}) for Cu increases with increasing Cu overlayer thickness. For the Cu/Ni(30 Å)/Cu/Ni/Cu(001) structures, the value of a_{in} of the 30-Å Ni film directly depends on a_{in} of the Cu underlayer. Magneto-optic Kerr effect measurements on a Cu/Ni/Cu/Ni₆₀Cu₄₀(001) structure reveal an increase in the magnetoelastic anisotropy with increasing Cu spacer layer thickness and, surprisingly, suggest no significant difference between the interface anisotropy of the Ni-Cu and the Ni-Ni₆₀Cu₄₀ interface. The stronger perpendicular magnetic anisotropy for Cu/Ni/Cu(001) structures compared to Cu/Ni/Ni₆₀Cu₄₀/Cu(001) is therefore attributed to an increased magnetoelastic anisotropy contribution.

Perpendicular magnetic anisotropy (PMA) has been observed in a wide range of ultrathin magnetic films. Heteroepitaxial systems that show PMA include fcc Fe/Cu(001),¹⁻⁴ bcc Fe/Ag(001),^{5,6} Co/Pd superlattices,^{7,8} and Co/Au(111) thin films and superlattices.⁹ In particular, epitaxial Cu/Ni/Cu(001) sandwiches show PMA over a large thickness range from about 25 to 140 Å.¹⁰⁻¹⁵ In order to gain an understanding of the PMA, an independent determination of the magnitudes of the contributions to the total magnetic anisotropy energy, such as shape, magneto-crystalline, magnetoelastic, and interface anisotropy is crucial. The magnetic film thickness dependence (t) of the effective magnetic anisotropy energy (K_{eff}) is often separated into a bulk magnetic anisotropy (K^V) and an interface contribution (K^S):

$$K^{\text{eff}} = K^V + 2K^S/t. \quad (1)$$

K^V includes the magnetostatic energy, the bulk magnetocrystalline energy (K_{MC}^b), and the magnetoelastic anisotropy, respectively. K^S includes the Néel-type interface anisotropy (K^N),¹⁶ originating in the broken symmetry of the interface atoms. It has been furthermore proposed that a strain dependent part of the interface anisotropy, i.e., the surface magnetoelastic anisotropy, should be included into the interface anisotropy;^{15,17} K^{eff} can then be described as

$$K^{\text{eff}} = -2\pi M_S^2 + K_{\text{MC}}^b + B^b \epsilon + (K^N + B^s \epsilon)/t. \quad (2)$$

Here B^b and B^s are the bulk and surface magnetoelastic coupling coefficient, ϵ the strain tensor, and M_S the saturation magnetization. Magnetoelastic anisotropy energies have been found to be different to the bulk for several systems, such as polycrystalline NiFe/Ag/Si, FeNi/Cu/Si thin films¹⁷ and Ni/Ag multilayers.^{17,18} For Cu/Ni/Cu(001) structures a

double transition of the magnetic anisotropy with Ni thickness has been found.^{10,15} For Ni thicknesses above about 140 Å, an in-plane magnetization is found due to the dominant shape anisotropy.¹⁰ In the range from about $25 < t < 140$ Å an out-of-plane magnetization is found. This is attributed to the magnetoelastic anisotropy of the strained Ni film due to the lattice mismatch to the Cu(001) substrate.^{10,15,19,20} Ni films on Cu(001) show for the first few monolayers an a_{in} expansion due to the Ni-Cu lattice mismatch which is accompanied by a contraction of the interlayer spacing.^{21,22} With increasing Ni film thickness the strain is released via misfit dislocations.²³ In the Ni thickness range below 25 Å, an in-plane magnetization occurs which has been interpreted differently:

(i) It has been argued that the Ni-Cu interface shows a negative K^N causing the in-plane magnetization in this thickness range.^{10,11} This is supported by the results of recent band-structure calculations, which yield a negative K^N for Cu/Ni/Cu(001) sandwiches.²⁴

(ii) On the other hand, it has been argued that the Ni-Cu interface shows a positive K^N and a large negative surface magnetoelastic coupling energy B^S .^{13,15} The PMA for Cu/Ni/Cu(001) sandwiches for $25 < t < 140$ Å is explained to originate from the bulk magnetocrystalline anisotropy $B^b \epsilon$ and the positive surface anisotropy K^N , whereas the in-plane magnetization found up to 25 Å is caused by a large negative B^S .

Experimental evidence for a positive K^N has been obtained from magnetic anisotropy behavior Ni/Cu_{1-x}Ni_x/Cu(001) structures.¹³ Ni/Cu_{1-x}Ni/Cu(001) thin films show a transition from an out-of-plane easy axis to an in-plane easy axis of magnetization with increasing Ni content of the Ni-Cu alloy substrate.¹³ This behavior has

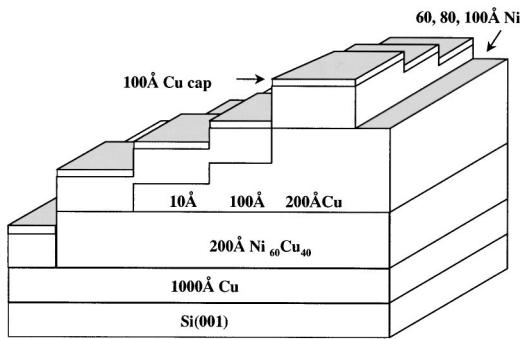


FIG. 1. Schematic diagram of the sample structure. The actual size of the sample is 2×2 cm.

been assumed to be attributed to a change of K^N at the Ni-Cu $_{1-x}$ Ni $_x$ interface with Ni content, whereas the differences in the lattice mismatch has been assumed to have no effect on the PMA.

In view of the controversy on the origin of the layer thickness dependent magnetic anisotropy of Ni/Cu(001) films we have here studied the PMA and a_{in} of an epitaxial Cu/Ni/Cu/Ni $_{60}$ Cu $_{40}$ /Cu(001) structure (sample 1) and a Ni(30 Å)/Cu/Ni/Cu(001) structure (sample 2). By varying the Ni and Cu spacer layer thickness we can systematically modulate the lattice mismatch and the chemical composition at the interface of the Ni films, and thereby study the effect of these parameters on the PMA.

Reflection high-energy electron-diffraction (RHEED) measurements reveal that for the Cu/Ni/Cu/Ni $_{60}$ Cu $_{40}$ /Cu(001) structure and Ni(30 Å)/Cu/Ni/Cu(001) structures, the a_{in} for Cu increases with increasing Cu spacer layer thickness and that for the 30-Å-thick Ni film, a_{in} directly depends on the a_{in} of the Cu spacer layer. Polar magneto-optic Kerr effect (MOKE) measurements on the Cu/Ni/Cu/Ni $_{60}$ Cu $_{40}$ (001) structure reveal an increase in the magnetoelastic anisotropy strength with increasing Cu spacer layer thickness and surprisingly suggest no significant difference between the interface anisotropy of the Ni-Cu and the Ni-Ni $_{60}$ Cu $_{40}$ interface. We conclude from our measurements that there is no evidence for a strong positive Néel-type interface anisotropy in the Cu/Ni/Cu(001) system in contrast with previous suggestions.¹⁵

Figure 1 shows a schematic diagram of the staircases structure (sample 1) prepared for this study. From the left- to the right-hand sides are shown a region where the Ni film is (a) directly grown onto Cu/Si(001), (b) onto Ni $_{60}$ Cu $_{40}$ (200 Å)/Cu/Si(001), (c)–(e) on a Cu staircase (10-, 100-, 200-Å Cu)/Ni $_{60}$ Cu $_{40}$ (200 Å)/Cu/Si(001) structure, and (e) 200-Å Cu/Ni $_{60}$ Cu $_{40}$ (200 Å)/Cu/Si(001). The Ni film is grown as a staircase with three different thickness of 60, 80, and 100 Å, as also illustrated in Fig. 1. The Si(001) substrates were etched in diluted hydrogen fluoride solution for 12 min prior to loading into the growth chamber and annealed for 2 h at ~ 200 °C after overnight bakeout. The samples were prepared using ultrahigh vacuum vapor deposition at ambient temperatures. Cu was evaporated using an electron-beam-heated Mo crucible, while Ni evaporation was done by electron-beam heating of the Ni rod. The base pressure of the chamber was 4×10^{-10} mbars for the growth of sample 1. The pressure increased during deposition for the Cu films to 2

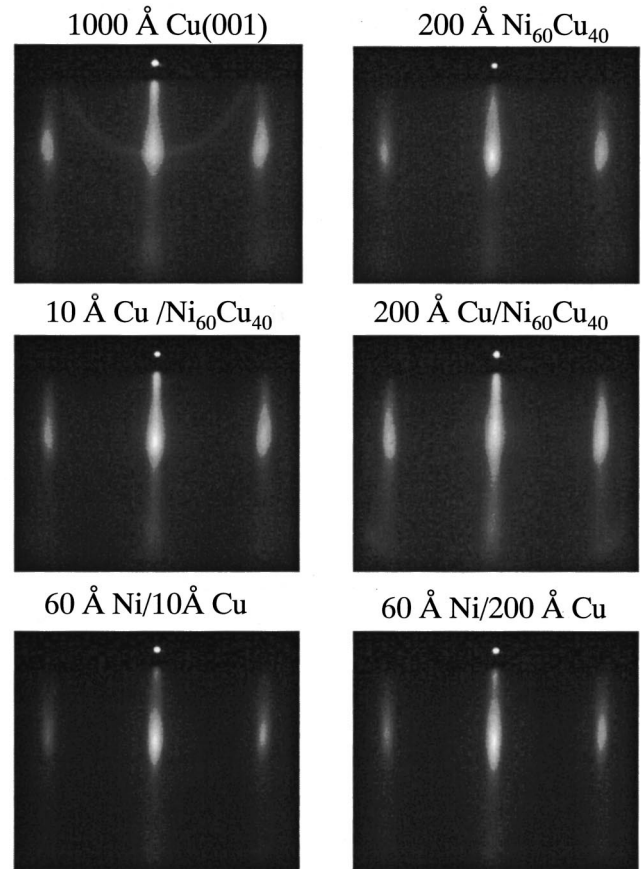


FIG. 2. RHEED images along the $\langle 100 \rangle$ Cu azimuth of 1000-Å Cu(001), Ni $_{60}$ Cu $_{40}$ (200 Å)/Cu(001), Cu(10,200 Å)/Ni $_{60}$ Cu $_{40}$ /Cu(001), and Ni(60 Å)/Cu(10,200 Å)/Ni $_{60}$ Cu $_{40}$ /Cu(001) grown on Si(001). The RHEED images are qualitatively very similar, confirming the epitaxial growth of the consecutive layers.

$\times 10^{-9}$ mbars, while it was maintained in the mid- 10^{-10} -mbars range during deposition of the Ni and Ni $_{60}$ Cu $_{40}$ film. A 1000-Å-thick Cu buffer was grown at ~ 7 Å/min. The 200-Å Ni $_{60}$ Cu $_{40}$ layer was grown by codeposition at ~ 4 Å/min. A Cu staircase (10, 100, and 200 Å) was grown on part of the Ni $_{60}$ Cu $_{40}$ film. The sample was then rotated by 90° and a Ni staircase (60, 80, and 100 Å) was grown at ~ 2 Å/min. The Ni film is capped with a 100-Å Cu film. The film thicknesses and growth rates were estimated using a quartz-crystal monitor close to the sample position. The cleanliness of the films were confirmed by Auger electron spectroscopy after completion of each film growth. The composition for the Ni $_{60}$ Cu $_{40}$ was furthermore checked by Auger electron spectroscopy. Furthermore a Cu/30-Å Ni/Cu (0–600 Å)/300-Å Ni/2000-Å Cu/Si(001) was grown (sample 2) under similar growth condition. RHEED images were taken after the completion of each layer on each step of the staircase structure, by translating the sample, but without changing other conditions, such as the direction of the electron beam. The images are recorded with a digital camera.

Figure 2 shows typical RHEED images taken after the completion of the growth of the subsequent layers along the $\langle 100 \rangle$ Cu azimuth for sample 1. The [001] direction of the Cu and Ni cubic axes are rotated in plane by 45° with respect to the Si(001) principal axes.²⁵ After the deposition of the 1000-Å Cu film on Si(001), the RHEED pattern shows sharp

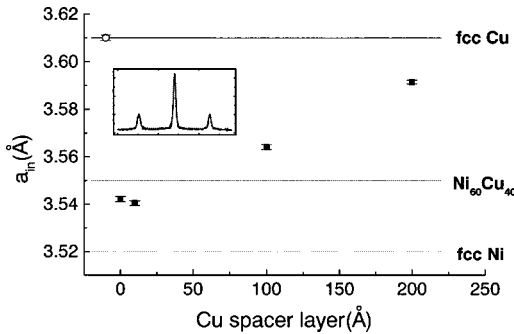


FIG. 3. In-plane lattice parameter for the Cu spacer/NiCu/1000-Å Cu/Si(001) structure with different spacer layer thickness (solid square) and the 1000-Å Cu/Si(001) structure (open circle). The bulk lattice parameters are indicated by the three lines. The inset shows the line profile of a 1000-Å Cu/Si(001), and the curve fitting to it.

and elongated spots or streaks. This indicates that the growth of Cu on Si(001) is epitaxial but dominated by three-dimensional growth, as previously reported.^{25–27} No large qualitative changes in the RHEED pattern are observed during the subsequent Ni₆₀Cu₄₀, Cu, and Ni film growth indicating their epitaxial relationship. We determined a_{in} from the streaks distance in the RHEED images through a line-shape analysis after the completion of the Cu spacer layer. The inset in Fig. 3 shows a typical line intensity profile of the RHEED image for the 1000-Å Cu/Si(001) and the fitted curves using three Gaussian functions. The absolute value of a_{in} is determined, by assuming a_{in} of the Cu buffer film to be bulklike. Figure 3 shows the result of this analysis for sample 1. For the Ni₆₀Cu₄₀(200 Å)/Cu(001) structure $a_{in}=3.54$ Å is determined, which is close to the bulk Ni₆₀Cu₄₀ in-plane lattice parameter of $a_{in}=3.55$ Å.²⁸

Cu is reported to grow epitaxially on Ni(001). The strain is reported to be relieved even from the first monolayers by internal (111) faceting, whereas for larger thicknesses (from about 18 monolayers) the strain is relieved via misfit dislocations.^{29–32} A similar behavior might be also expected for Cu on Ni₆₀Cu₄₀(001). Therefore already for 10-Å Cu film on Ni₆₀Cu₄₀(001) film a_{in} of Cu might slightly deviate from that of the Ni₆₀Cu₄₀(001) film.

However, within experimental resolution, the a_{in} of the 10-Å Cu/Ni₆₀Cu₄₀ and the Ni₆₀Cu₄₀ film are found to be very similar. With increasing thickness the Cu a_{in} relaxes towards the bulk Cu lattice constant. For the case of the 100-Å Cu/Ni₆₀Cu₄₀ and the 200-Å Cu/Ni₆₀Cu₄₀, the a_{in} is determined to be 3.56 and 3.59 Å, respectively. Therefore we can continuously modulate the a_{in} of the Cu layer by growing it on a Ni₆₀Cu₄₀/Cu(001) film. This further allows one to engineer the lattice mismatch between a Ni film to the Cu underlayer, and to study its influence on the perpendicular magnetic anisotropy for Ni/Cu(001) structures. The bulk Ni-Cu phase diagram indicates that Ni and Cu form a solid solution, which is nonmagnetic at room temperature, provided the Ni content is less than 65 at.%.²⁸ In our experiment we therefore used a Ni₆₀Cu₄₀ film, which should be nonmagnetic, as we also confirmed by polar MOKE measurements.

We have furthermore determined the a_{in} for a Ni (30 Å)/Cu(0–600 Å)/Ni/Cu/Si(001) structure from a line-profile

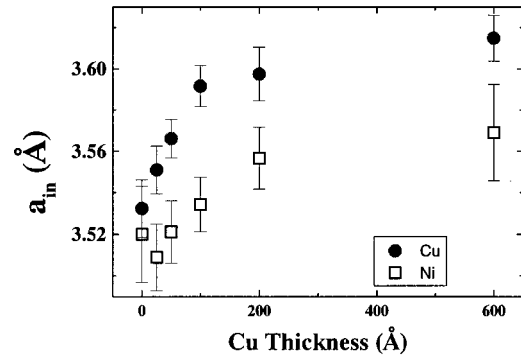


FIG. 4. In-plane lattice parameter for the Cu (0–600 Å)/Ni(300 Å)/Cu(001) and 30-Å Ni/(0–600 Å) Cu/Ni (300 Å)/Cu(001) structure for different Cu layer thicknesses.

analysis of the RHEED images. RHEED images have been taken for each Cu spacer layer thickness both after the completion of the Cu spacer layer, and after the completion of the 30-Å Ni overlayer. This allows us to study the a_{in} of the Ni film in relation to the lattice mismatch of the Cu underlayer. The results of this analysis are shown in Fig. 4. We find that a_{in} for both Cu and Ni overlayers increases with increasing Cu spacer layer thickness. For the 30-Å Ni layer, a_{in} is found to be smaller than for Cu for all Cu spacer layer thicknesses. This directly shows that the 30-Å Ni is partly relaxed in each case. The lateral strain in the Ni overlayer is largest when grown on the 600-Å Cu spacer layer and approximately follows the lateral strain of the Cu/Ni/Cu(001) structure.

Figure 5 shows the polar MOKE hysteresis loops for Cu/Ni(10, 100, 200 Å) Cu/Ni₆₀Cu₄₀/Cu(001) structures with different Ni layer thicknesses. The hysteresis curves for the Ni/100-Å Cu/Ni₆₀Cu₄₀ and the Ni/200-Å Cu/Ni₆₀Cu₄₀ are very similar to each other for each Ni thickness. The Ni/10-Å Cu/Ni₆₀Cu₄₀ structures show a relatively lower remanence and lower saturation field compared to those of the Ni/100 Å

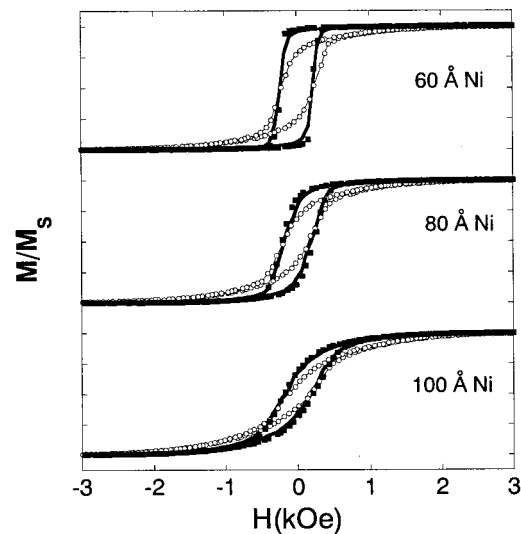


FIG. 5. Polar MOKE hysteresis loops of (—) Cu/Ni/10-Å Cu, (---) Cu/Ni/100-Å Cu, and (■) Cu/Ni/200-Å Cu on Ni₆₀Cu₄₀/Cu(001) for different Ni layer thicknesses. The loops are normalized at saturation and shifted for different Ni thicknesses for clarity.

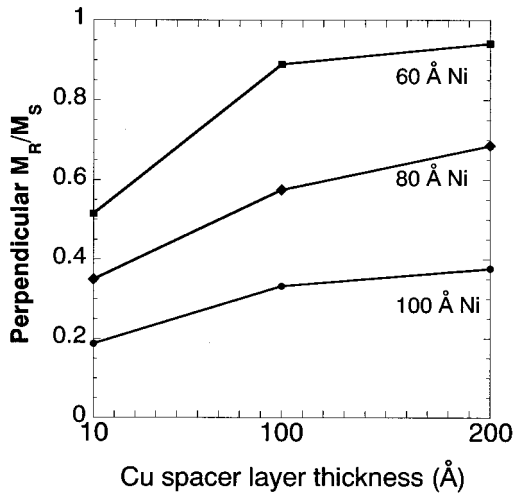


FIG. 6. Perpendicular remanence determined from polar MOKE measurements, as shown in Fig. 4, for the Cu/Ni/Cu spacer/ $\text{Ni}_{60}\text{Cu}_{40}/\text{Cu}(001)$ structure.

$\text{Cu}/\text{Ni}_{60}\text{Cu}_{40}$ and $\text{Ni}/200\text{-}\text{\AA}\text{ Cu}/\text{Ni}_{60}\text{Cu}_{40}$ structures for the three different Ni thicknesses. Figure 6 shows the perpendicular remanence determined from these polar MOKE measurements. The remanence is found to gradually increase with increasing Cu spacer layer thickness and to gradually decrease with increasing Ni layer thickness. This behavior together with the observed changes in the perpendicular saturation field suggests that the PMA increases with increasing Cu spacer layer thickness, and decreases with increasing Ni layer thickness. We previously found that for $\text{Cu}/\text{Ni}/\text{Cu}/\text{Si}(001)$ structures the magnetic moment is close to its bulk value for Ni thickness above around 50 \AA .^{33–35} Therefore we would not expect the changes observed in the magnetic anisotropy behavior for the $60\text{-}\text{\AA}$ Ni films investigated here to be largely affected by possible variations in the magnetic moments but rather dominated by the influence of the lattice misfit on the PMA of the $\text{Ni}/\text{Cu}(001)$ films. With increasing Cu spacer layer thickness, the Ni-Cu lattice mismatch of the Ni film increases. This causes an increase in the magnetoelastic anisotropy energy and therefore PMA. The $\text{Cu}/60\text{-}\text{\AA}\text{ Ni}/200\text{-}\text{\AA}\text{ Cu}/\text{Ni}_{60}\text{Cu}_{40}/\text{Cu}(001)$ structure shows an almost completely square loop, indicating PMA. For the $200\text{-}\text{\AA}$ Cu film a_{in} is nearly the same as for the bulk value of $\text{Cu}(001)$, as shown in Fig. 3. The $\text{Cu}/60\text{-}\text{\AA}\text{ Ni}/200\text{-}\text{\AA}\text{ Cu}/\text{Ni}_{60}\text{Cu}_{40}/\text{Cu}(001)$ is therefore expected to show a magnetic anisotropy behavior similar to that of a $\text{Cu}/60\text{-}\text{\AA}\text{ Ni}/\text{Cu}(001)$ structure which is reported to show PMA.^{10,15,22,25,36} The polar MOKE curve for the $\text{Cu}/60\text{-}\text{\AA}\text{ Ni}/200\text{-}\text{\AA}\text{ Cu}/\text{Ni}_{60}\text{Cu}_{40}/\text{Cu}(001)$ is very similar to that of the $\text{Cu}/60\text{-}\text{\AA}\text{ Ni}/\text{Cu}(001)$ sandwich (shown in Fig. 8) confirming this view. In the incoherent growth regime a_{in} gradually relaxes to its bulk value with increasing Ni thickness causing a decreasing influence of the magnetoelastic anisotropy on the PMA.^{10,15,23,36,37}

We have shown that the a_{in} for the $\text{Cu}(10\text{ \AA})/\text{Ni}_{60}\text{Cu}_{40}/\text{Cu}(001)$ film is within error the same as that of $\text{Ni}_{60}\text{Cu}_{40}/\text{Cu}(001)$ film. It is therefore interesting to investigate the magnetic anisotropy for $\text{Cu}/\text{Ni}/\text{Ni}_{60}\text{Cu}_{40}/\text{Cu}(001)$ and $\text{Cu}/\text{Ni}/10\text{-}\text{\AA}\text{ Cu}/\text{Ni}_{60}\text{Cu}_{40}/\text{Cu}(001)$ structures. This allows us to directly compare K^N of the Ni-Cu and the

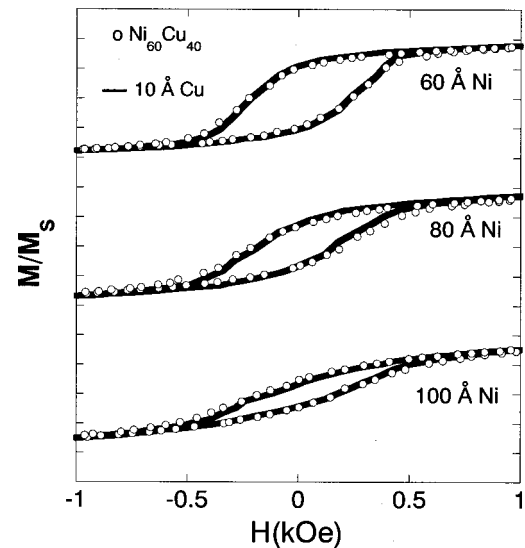


FIG. 7. Polar MOKE hysteresis loops of (o) $\text{Cu}/\text{Ni}/\text{Ni}_{60}\text{Cu}_{40}/\text{Cu}(001)$ and (—) $\text{Cu}/\text{Ni}/10\text{-}\text{\AA}\text{ Cu}/\text{Ni}_{60}\text{Cu}_{40}/\text{Cu}(001)$ structures for different Ni layer thicknesses as indicated in the graph. The loops are normalized at saturation and shifted for clarity.

$\text{Ni}-\text{Ni}_{60}\text{Cu}_{40}$ interface, since only very small differences in the magnetoelastic volume anisotropy contribution is expected between such structures. Figure 7 shows the polar MOKE hysteresis curves for $\text{Cu}/\text{Ni}/10\text{-}\text{\AA}\text{ Cu}/\text{Ni}_{60}\text{Cu}_{40}/\text{Cu}(001)$ and $\text{Cu}/\text{Ni}/\text{Ni}_{60}\text{Cu}_{40}/\text{Cu}(001)$ structures of different Ni layer thicknesses. Surprisingly the hysteresis loops of the $\text{Cu}/\text{Ni}/\text{Ni}_{60}\text{Cu}_{40}$ are the same as for the $\text{Cu}/\text{Ni}/10\text{-}\text{\AA}\text{ Cu}/\text{Ni}_{60}\text{Cu}_{40}$ sample for each Ni thickness, respectively. Therefore there is no indication that K^N of the Ni-Cu and the Ni- $\text{Ni}_{60}\text{Cu}_{40}$ interfaces are different. One explanation might be that the size of K^N of the Cu/Ni interface is relatively small in terms of K^{eff} , and slight changes in K^N between the Ni-Cu interface and the Ni- $\text{Ni}_{60}\text{Cu}_{40}$ interface would not be significant. Another interpretation is that the chemical composition of the $\text{Ni}_{60}\text{Cu}_{40}$ surface is actually more like a Cu surface due to surface segregation of the Cu atoms. Cu is well known to segregate to the surface for Cu-Ni alloys and alloy films for a wide range of compositions.^{38–41} Increasing the temperature tends to drive the Cu from the surface into the bulk. The Cu surface layer concentration for a $\text{Cu}_{50}\text{Ni}_{50}$ alloy has been calculated to be close to one at 400 K .³⁹ The $\text{Ni}_{60}\text{Cu}_{40}$ film in our experiment is relatively thick (200 \AA) and grown at room temperature. Therefore some Cu surface segregation is expected to occur.

Figure 8 shows the polar MOKE hysteresis curves for the $\text{Cu}/\text{Ni}/\text{Cu}(001)$ and $\text{Cu}/\text{Ni}/\text{Ni}_{60}\text{Cu}_{40}/\text{Cu}(001)$ structures for different Ni thicknesses. The $\text{Cu}/60\text{-}\text{\AA}\text{ Ni}/\text{Cu}(001)$ structure shows an almost completely square hysteresis loop indicating PMA. The $\text{Cu}/60\text{-}\text{\AA}\text{ Ni}/\text{Ni}_{60}\text{Cu}_{40}/\text{Cu}(001)$ structure shows a largely reduced remanence field, and an increased saturation field compared to the $\text{Cu}/60\text{-}\text{\AA}\text{ Ni}/\text{Cu}(001)$ structures. This shows that the PMA is weaker for Ni films grown on $\text{Ni}_{60}\text{Cu}_{40}/\text{Cu}(001)$ compared to those directly grown on $\text{Cu}(001)$. The difference in the remanence and perpendicular saturation field for the different spacer layer becomes smaller for the $80\text{-}\text{\AA}$ Ni film, while for the $100\text{-}\text{\AA}$ Ni film, the hys-

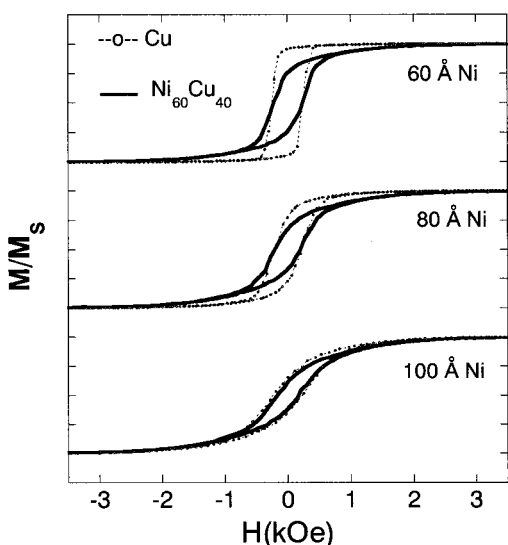


FIG. 8. Comparison of polar MOKE hysteresis loops of (-o-) Cu/Ni/Cu(001) and (—) Cu/Ni/Ni₆₀Cu₄₀/Cu(001) structures for three different Ni layer thicknesses as indicated in the graph. The loops are normalized at saturation and shifted for clarity.

teresis curves are almost the same for the Ni₆₀Cu₄₀(001) and Cu(001) underlayer. Two mechanisms are potentially important here: the interface anisotropy and strain. Since K^N for the Ni-Cu and Ni-Ni₆₀Cu₄₀ interface is not significantly different (see Fig. 7), the changes observed here in the effective magnetic anisotropy behavior for Cu/Ni/Cu(001) structures compared with Cu/Ni/Ni₆₀Cu₄₀(001) can be attributed to the difference in the magnetoelastic anisotropy. The lattice mismatch between Ni and Cu is 2.5% compared to only 1.1% between fcc Ni and the Ni₆₀Cu₄₀ alloy.²⁸ We have shown that incoherently grown Ni films are less strained, when the lattice mismatch to the Cu(001) underlayer is smaller. Therefore the magnetoelastic anisotropy becomes weaker, reducing the PMA for the Ni film when grown on Ni₆₀Cu₄₀/Cu(001) compared to when directly grown on Cu(001). With increasing Ni layer thickness, the Ni films become increasingly relaxed and differences in the magnetoelastic anisotropy become less important.

The magnetic anisotropy of Ni/CuNi/Cu(001) thin films has been previously investigated by Bochi *et al.* in order to qualitatively test the effect of K^N and the surface magnetoelastic anisotropy on the PMA in Ni/Cu(001) thin films.¹³

The region of PMA for Ni/Cu₆₀Ni₄₀/Cu(001) has been found to be narrower than for Ni/Cu(001) films. The perpendicular magnetic remanence is found to decrease with increasing Ni and to essentially vanish for Ni contents $X > 25\%$ for Ni(100 Å)/Cu_{1-x}Ni_x/Cu(001). Based on the Mathews-Blakeslee model⁴² the authors expect the misfit strain in the Ni film to be independent on the lattice mismatch to the underlayer in the incoherent growth regime. More recently it has been found, however, that for metal interface with square symmetry, such as Cu on Ni(001), strain can be already relieved in the submonolayer range,^{29,31} as also explained in more recent models on elastic strain relaxation.⁴³ Our observation that a_{in} for a Ni film directly depends on a_{in} of the Cu underlayer therefore is supported by recent experimental and theoretical studies. For Ni/CuNi/Cu(001) changes of the magnetic anisotropy with the Ni content have been attributed to differences of K^N for the Ni-Cu interface compared to the Ni-Cu_{1-x}Ni_x interface in Ref. 13. However, our MOKE measurements show the same magnetic anisotropy behavior for the Cu/Ni/Cu(10 Å)/Ni₆₀Cu₄₀(001) and the Cu/Ni/Cu(10 Å)/Ni₆₀Cu₄₀(001) structure. This suggests that K^N for the Ni-Cu interface and the Ni-Ni₆₀Cu₄₀ interface are not significantly different and therefore oppose the assumption made in Ref. 13.

In conclusion, we have studied the PMA and the in-plane lattice parameter of epitaxial Cu/Ni/Cu/Ni₆₀Cu₄₀/Cu(001) and Ni/Cu/Ni/Cu(001) structures as a function of the Ni and Cu spacer layer thickness. RHEED measurements reveal that the in-plane parameter of an Ni film epitaxially grown on Cu(001) directly depends on the lattice parameter of the Cu underlayer. MOKE measurements on a Cu/Ni/Cu/Ni₆₀Cu₄₀(001) structure directly reveal an increase in the magnetoelastic anisotropy and therefore perpendicular magnetic anisotropy with increasing Ni-Cu lattice mismatch and surprisingly suggest no significant difference between the interface anisotropy of the Ni-Cu and the Ni-Ni₆₀Cu₄₀ interface. We therefore attribute the stronger PMA found for Cu/Ni/Cu(001) structures compared with the Cu/Ni/Ni₆₀Cu₄₀/Cu(001) structures to a larger magnetoelastic anisotropy contribution.

This work was supported by the EPSRC (UK), the SPIDER (Esprit) and SUBMAGDEV (TMR) program of the EU, the Toyota School Foundation, and the Japanese Society of Promotion of Science. C. A. F. Vaz acknowledges support from JNICT.

¹D. Pescia, M. Stampanoni, G. L. Bona, A. Vaterlaus, and R. F. Willis, Phys. Rev. Lett. **58**, 2126 (1987).

²C. Liu, E. R. Moog, and S. D. Bader, Phys. Rev. Lett. **60**, 2422 (1988).

³D. P. Pappas, K.-P. Kämper, and H. Hopster, Phys. Rev. Lett. **64**, 3179 (1992).

⁴R. Allensbach and A. Bischoff, Phys. Rev. Lett. **69**, 3385 (1992).

⁵N. C. Koon, B. T. Jonker, F. A. Volkening, J. J. Krebs, and G. A. Prinz, Phys. Rev. Lett. **59**, 2463 (1987).

⁶B. Heinrich, K. B. Urquhart, A. S. Arrot, J. F. Cochran, K. Myrtle, and S. T. Purcell, Phys. Rev. Lett. **59**, 1756 (1987).

⁷B. N. Engel, C. D. England, R. A. Van Leeuwen, N. H. Wied-

mann, and C. M. Falco, Phys. Rev. Lett. **67**, 1910 (1991).

⁸F. J. A. den Broeder, W. Hoving, and P. J. H. Bloemen, J. Magn. Magn. Mater. **93**, 562 (1991).

⁹F. J. A. den Broeder, D. Kuiper, A. P. van de Mosselaer, and W. Hoving, Phys. Rev. Lett. **60**, 2769 (1988).

¹⁰R. Jungblut, M. T. Johnson, J. aan de Stegge, A. Reinders, and F. J. A. den Broeder, J. Appl. Phys. **75**, 6424 (1994).

¹¹W. L. O'Brien, T. Droubay, and B. P. Tonner, Phys. Rev. B **54**, 9297 (1996).

¹²P. Rosenbusch, J. Lee, G. Lauhoff, and J. A. C. Bland, J. Magn. Magn. Mater. **172**, 19 (1997).

¹³G. Bochi, C. A. Ballentine, H. E. Inglefield, C. V. Thompson, R.

- C. O'Handley, and H. J. Hug, Phys. Rev. B **52**, 7311 (1995).
- ¹⁴G. Bochi, H. J. Hug, D. I. Paul, A. Moser, I. Parashikov, H.-J. Güntherodt, and R. C. O'Handley, Phys. Rev. Lett. **75**, 1839 (1995).
- ¹⁵G. Bochi, C. A. Ballentine, H. E. Inglefield, C. V. Thompson, and R. C. O'Handley, Phys. Rev. B **53**, R1729 (1996).
- ¹⁶M. L. Néel, J. Phys. Radium **15**, 225 (1954).
- ¹⁷R. C. O'Handley, O. Song, and C. A. Ballentine, J. Appl. Phys. **74**, 6302 (1993).
- ¹⁸H. Szymczak, J. Appl. Phys. **81**, 5411 (1997).
- ¹⁹B. Schulz and K. Baberschke, Phys. Rev. B **50**, 13 467 (1994).
- ²⁰W. L. O'Brien and B. P. Tonner, Phys. Rev. B **49**, 15 370 (1994).
- ²¹W. Platow, U. Bovensiepen, P. Pouloupoulos, M. Farle, and K. Baberschke, Phys. Rev. B **59**, 12 641 (1999).
- ²²C.-A. Chang, J. Appl. Phys. **68**, 4873 (1990).
- ²³H. E. Inglefield, C. A. Ballentine, G. Bochi, S. S. Bogomolov, and R. C. O'Handley, in *Thin Films: Stresses and Mechanical Properties IV*, edited by P. H. Townsend, T. P. Weihs, J. E. Sanchez, Jr., and P. Børgeesen, MRS Symposia Proceedings No. 308 (Materials Research Society, Pittsburgh, 1993), p. 765.
- ²⁴G. Y. Guo, J. Magn. Magn. Mater. **176**, 97 (1997).
- ²⁵R. Naik, C. Kota, J. S. Payson, and G. L. Dunifer, Phys. Rev. B **48**, 1008 (1993).
- ²⁶R. Naik, M. Ahmad, G. L. Dunifer, C. Kota, A. Poli, K. Fang, U. Rao, and J. S. Payson, J. Magn. Magn. Mater. **121**, 60 (1993).
- ²⁷B. G. Demczyk, R. Naik, G. Auner, C. Kota, and U. Rao, J. Appl. Phys. **75**, 1956 (1994).
- ²⁸R. M. Bozorth, *Ferromagnetism* (IEEE Press, New York, 1993), p. 308.
- ²⁹B. Müller, B. Fischer, L. Nedelmann, A. Fricke, and K. Kern, Phys. Rev. Lett. **76**, 2358 (1996).
- ³⁰B. Müller, L. Nedelmann, B. Fischer, A. Fricke, and K. Kern, J. Vac. Sci. Technol. A **14**, 1878 (1996).
- ³¹L. Nedelmann, B. Müller, B. Fischer, K. Kern, D. Erdö, J. Wollschläger, and M. Henzler, Surf. Sci. **376**, 113 (1997).
- ³²R. Kern and P. Müller, Surf. Sci. **392**, 103 (1997).
- ³³J. Lee, G. Lauhoff, G. Fermon, S. Hope, J. A. C. Bland, J. P. Schille, G. van der Laan, C. Chappert, and P. Beauvillain, J. Phys.: Condens. Matter **9**, L137 (1997).
- ³⁴G. Lauhoff, J. A. C. Bland, J. Lee, J. P. Schille, and G. van der Laan, Phys. Rev. B **60**, 4087 (1998).
- ³⁵G. Lauhoff, J. Lee, J. A. C. Bland, J. P. Schille, and G. van der Laan, J. Magn. Magn. Mater. **177**, 1253 (1998).
- ³⁶J. Lee, G. Lauhoff, and J. A. C. Bland, Europhys. Lett. **35**, 463 (1996).
- ³⁷J. Lee, G. Lauhoff, M. Tselepi, S. Hope, P. Rosenbusch, J. A. C. Bland, H. A. Dürr, G. van der Laan, J. Ph. Schille, and J. A. D. Matthew, Phys. Rev. B **55**, 15 103 (1997).
- ³⁸S. Swaminarayan, R. Najafabadi, and D. J. Srolovitz, Acta Mater. **45**, 1715 (1997).
- ³⁹H. Y. Wang, R. Najafabadi, and D. J. Srolovitz, Phys. Rev. B **45**, 12 028 (1992).
- ⁴⁰T. Schulthess, R. Monnier, and S. Crampin, Phys. Rev. B **50**, 18 564 (1994).
- ⁴¹T. Sakurai, T. Hashizume, A. Jimbo, and A. Sakai, Phys. Rev. Lett. **55**, 514 (1985).
- ⁴²J. Y. Tsao, *Materials Fundamentals of Molecular Beam Epitaxy* (Academic, London, 1993), p. 151.
- ⁴³R. Kern and P. Müller, Surf. Sci. **392**, 103 (1997).